Published in Journal of Applied Physics 87, issue 6, 3137-3142, 2000
which should be used for any reference to this work

Evolution of the microstructure in microcrystalline silicon prepared by very high frequency glow-discharge using hydrogen dilution

E. Vallat-Sauvain, U. Kroll, J. Meier, and A. Shah
Institut de Microtechnique, Université de Neuchâtel, rue Breguet 2, 2000 Neuchâtel, Switzerland

J. Pohl
Universität Konstanz, D-78434 Konstanz, Germany

A series of samples was deposited by very high frequency glow discharge in a plasma of silane diluted in hydrogen in concentrations $SiH_4/(SiH_4+H_2)$ varying from 100% to 1.25%. For silane concentrations below 8.4%, a phase transition between amorphous and microcrystalline silicon occurs. Microcrystalline silicon has been characterized by transmission electron microscopy (TEM) and x-ray diffraction. The medium-resolution TEM observations show that below the transition, the microstructure of microcrystalline silicon varies in a complex way, showing a large variety of different growth structures. For the sample close to the phase transition, one observes elongated nanocrystals of silicon embedded in an amorphous matrix followed at intermediate dilution by dendritic growth, and, finally, at very high dilution level, one observes columnar growth. X-ray diffraction data evidence a (220) crystallographic texture; the comparison of the grain sizes as evaluated from TEM observations and those determined using Scherrer's equation illustrates the known limitations of the latter method for grain size determination in complex microstructures.

I. INTRODUCTION

Although hydrogenated microcrystalline silicon (μc-Si:H) prepared by plasma enhanced chemical vapor deposition (PECVD) is known from the work of Veprek and Marecek[1] since 1968, it has only recently appeared on the research scene as a promising new thin-film intrinsic material for device applications.[2–4] Since its discovery, the use of μc-Si:H as an intrinsic device grade material was not seriously taken into account. Undoped as-deposited layers exhibited a *n*-type character and due to its many small grains, this material was believed to have too high defect densities. By applying the very high frequency glow-discharge (VHF-GD) deposition technique, intrinsic μc-Si:H has been shown to be a very promising new photovoltaic material for thin-film (<10 μm) solar cells,[3] whereas intrinsic μc-Si:H deposited with an admixture of SiF_4 gas has been successfully incorporated into thin film transistors (TFTs).[4] In contrast with the excellent device performances obtained entirely for μc-Si:H solar cell devices and transistors, relatively little is known about the material microstructural properties.[5,6] Indeed, the link between thin-film microstructure and device performance is still far from being elucidated.

In practice, the dilution level of silane in hydrogen is one of the key parameters for the deposition of intrinsic μc-Si:H. The aim of our work is to study the effect of the variation of this parameter on the microstructure of layers, in the range used in practice for the deposition of solar cells. In the present study, transmission electron microscopy (TEM) yields qualitative information about the shape and crystallographic orientation of crystallites (or grains) in the material. The TEM micrographs reveal a striking diversity in layer microstructure that was not suspected from previous measurements. Furthermore, quantitative TEM grain size measurements will be compared here in detail with data evaluated from x-ray diffraction measurements previously published,[7] i.e., with the average size of x-ray coherent domains as calculated from Scherrer's equation.

II. EXPERIMENT

Films were deposited in a capacitively coupled parallel plate reactor using a plasma excitation frequency of 70 MHz. The silane concentration in the feed gas was varied from 100% down to 1.25% by adapting the ratio of the silane and hydrogen flows, while keeping the total feed gas constant at 50 sscm. The depositions were performed at a pressure of 0.4 mbar, a HF power input of 7 W, and a substrate temperature of 225 °C. Under these conditions, 1.5–2 μm thick films have been deposited on Corning 7059 glass substrate. For comparison, *i* layers incorporated in fully microcrystalline solar cells have thicknesses in this range.[3] This series has already been extensively characterized by infrared spectroscopy, elastic recoil detection analysis (ERDA), and x-ray diffraction.[7,8] These previous studies allowed us to determine the growth rate[7] and the hydrogen incorporation in the deposited layers,[8] as well as to locate the amorphous-microcrystalline phase transition.[7,8]

Electron-transparent samples for TEM characterization are usually prepared by the ion-milling thinning method. This method is known to amorphize silicon nanocrystals and to preferentially etch around cracks.[9] In order to minimize the effect of such preparation artefacts, we carefully scraped the films from the glass substrate and directly picked the fragments on a carbon-coated TEM grid. The grids were examined in a Philips CM200 electron microscope operated at

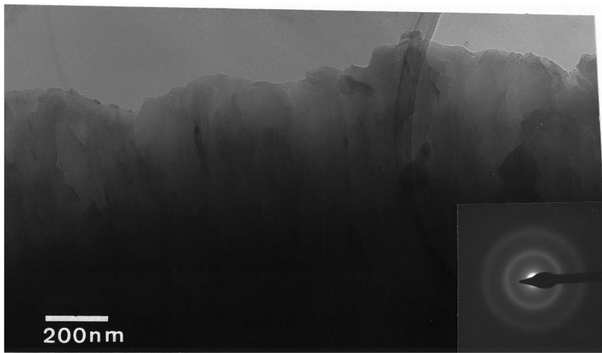

FIG. 1. Cross-section bright-field micrograph of the sample prepared at a silane concentration of 8.6%. The diffuse rings in the selected-area diffraction pattern (in inset) reveal the sample's amorphous nature. A columnar microstructure is visible in this sample.

an accelerating voltage of 200 kV. X-rays diffraction measurements were performed on a Siemens D501 powder diffractometer using the Bragg–Brentano configuration (θ–2θ scans). An accelerating voltage of 40 kV at 30 mA is used to produce Cu K_{α_1} radiation at a wavelength of 1.5406 Å.

III. RESULTS AND DISCUSSION

A. TEM observations

Figure 1 shows the cross section of a sample prepared at a silane concentration of 8.6%. The diffuse rings in the selected area diffraction pattern (in inset) are indicative of the sample's amorphous nature, and the bright-field micrograph gives evidence of a columnar microstructure.

Bright-field electron micrographs of the 7.5% dilution sample are given in Fig. 2. These micrographs reveal elongated nanocrystallites embedded in an amorphous tissue. From quantitative image analysis of Fig. 2(a) micrograph, we measured that the average grain size is 10 nm (standard deviation ±4 nm) and the surface crystalline fraction is approximatively 10%. As the crystallites have a length of the order of the estimated thickness of the electron transparent edge, we can approximate the volume crystalline fraction to the measured surface crystalline fraction. From optical measurements,[7] this sample has an absorption curve that lies in between the absorption curves for microcrystalline and for amorphous silicon. On the other hand, only a very faint x-rays signal indicative of crystallinity is observed (see Fig. 6). Optical absorption measurements seem, thus, to be more sensitive to the crystalline phase than x rays.

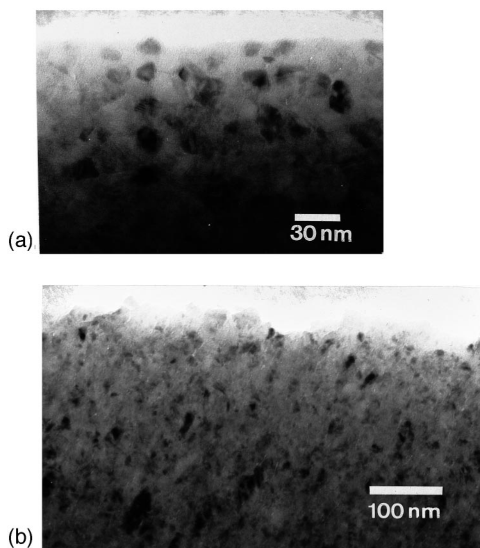

FIG. 2. (a) Plane-view bright-field micrograph of the sample prepared at a silane concentration of 7.5%. It exhibits small crystallites (10 nm average diameter, ±4 nm standard deviation) embedded in an amorphous matrix. (b) Side-view bright-field micrograph obtained under 30° tilt. It reveals the elongated shape of the crystallites (30 nm long).

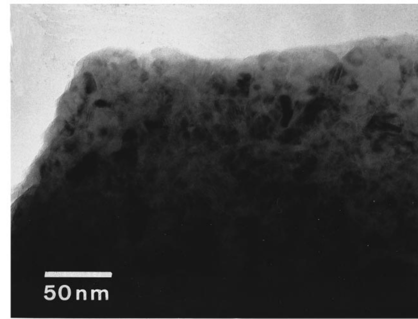

FIG. 3. Plane-view bright-field micrograph of the sample prepared at a silane concentration of 5%. The average diameter of the crystallites is 9 ±8 nm. About 15% of the surface is crystalline.

Figure 3 shows a plane-view micrograph of the 5% silane concentration sample. Like the 7.5% sample, it consists of elongated (cross section is not shown here) nanocrystallites embedded in an amorphous matrix. The quantitative analysis of Fig. 3 yields an average crystallite diameter of 9 nm (standard deviation ±8 nm) and a surface crystalline fraction of 15%. X-ray diffraction measurements reveal that a pronounced ⟨220⟩ preferential growth direction exists in this sample (see Fig. 7). We compared TEM dark-field images obtained either from the (111) or from the (220) diffraction ring. Dark-field micrographs from the latter reveal many more bright (diffracting) grains. Thus, our TEM observations confirm qualitatively the existence of a crystallographic texture in this sample.

Figures 4(a)–4(c) show the microstructure of the 2.5% silane concentration sample. We can observe grains of 28 nm average diameter (standard deviation ±28 nm), packed into bunches that have a total diameter of hundreds nanometers. The residual amorphous fraction in this sample (as well as in the higher dilution samples) could no longer be estimated from our medium-resolution TEM micrographs. The large bunches of grains in this sample are loosely packed. They result in a rough sample to air interface. One can observe another characteristic feature: leaf-like grains pointing out of the sample's surface. These are rather large monocrystals (150 nm diameter, 350 nm long) with a central symmetry axis consisting of a stacking fault. A surprisingly similar microstructure had already been observed in different thermally recrystallized amorphous silicon samples for TFT applications.[10,11] This observation may be of importance for the recently demonstrated application of as-deposited μc-Si:H in complementary metal–oxide–semiconductor

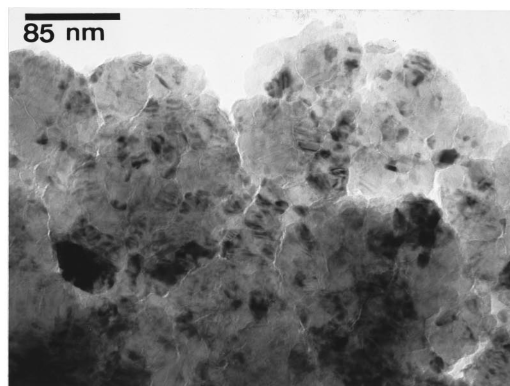

(a)

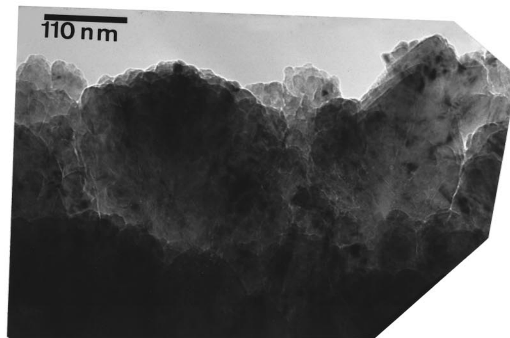

(b)

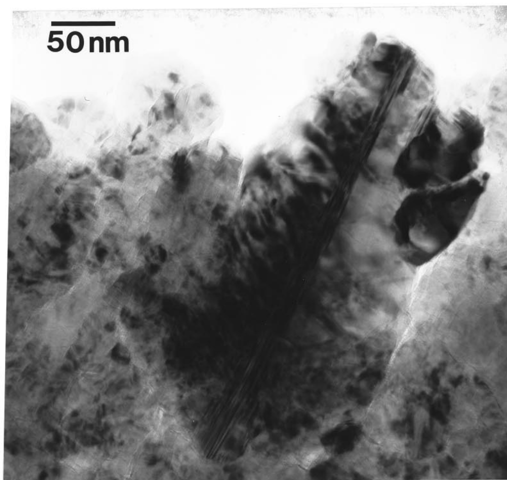

(c)

FIG. 4. (a) Plane-view bright-field micrograph of the sample prepared at a silane concentration of 2.5%. It consists of large (200 nm diameter) clusters of grains (average diameter 28 nm, standard deviation ±28 nm). The large clusters are loosely connected. (b) Cross-section bright-field micrograph exhibiting the large (200 nm diameter) bunches of grains, resulting in a rough sample-air interface. Single leaf-like-shaped grains pointing out of the sample can be identified [see (c)]. (c) A leaf-shaped grain pointing out of the sample. It shows a central symmetry axis, consisting of a planar defect.

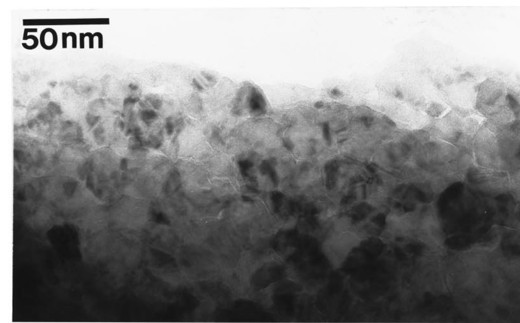

(a)

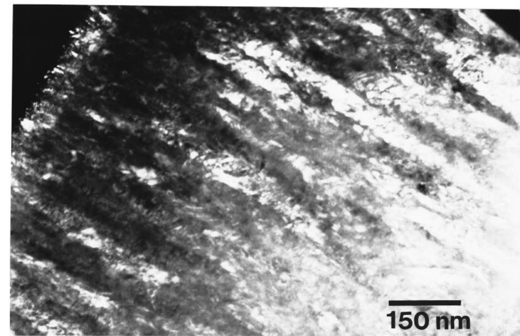

(b)

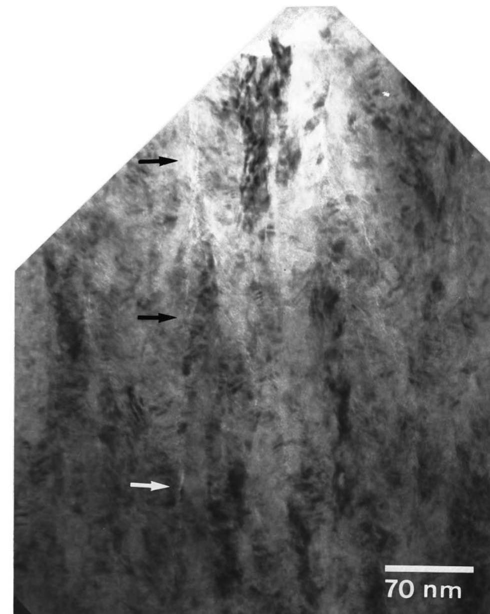

(c)

FIG. 5. (a) Plane-view bright-field micrograph of the sample prepared at a silane concentration of 1.25%. It shows loosely packed hexagonal grains of 20 nm diameter. (b) Cross-section dark-field micrograph. Columnar grains of 750 nm length can be observed. The microstructure over the first 40 nm close to the substrate-layer interface (upper left corner) is different: it exhibits a much smaller grain size distribution. (c) Cross-section bright-field micrograph. A crack running all the way through (460 nm) is indicated with arrows.

(CMOS) transistors.[4] This microstructure results from a specific recrystallisation mechanism: dendritic growth with a pronounced (220) crystallographic texture has been suggested in Ref. 10. But which growth mechanism in the plasma phase leads to such a dendritic microstructure in our sample remains unknown.

The natural, as-grown surface roughness of this sample has been investigated by atomic force microscopy (AFM). The surface root-mean-square roughness is $S_q = 18$ nm; such a rough surface leads to strong optical light scattering. This effect is very important when the layer is incorporated into a

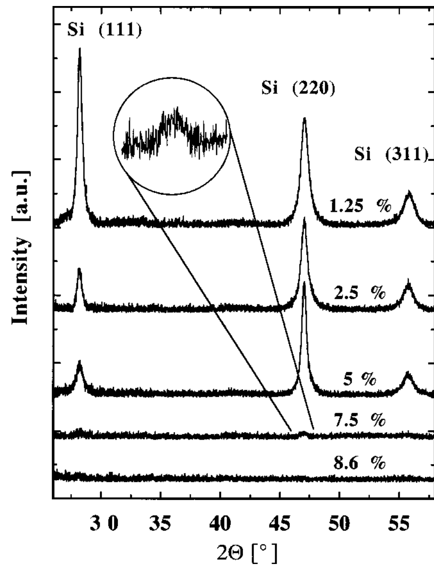

FIG. 6. X-ray diffraction spectra of the dilution series. The spectra are shifted vertically for better clarity.

solar cell as it results in an enhanced light trapping, and thus leads to an increased short-circuit current.[12]

The microstructure of the 1.25% dilution sample is represented in Fig. 5. It shows long (750 nm length), hexagonal (20 nm diameter) columnar grains, with an extremely rough surface (AFM root-mean-square value $S_q = 40\,\mathrm{nm}$). Cracks running a long way down the grains are present. Our medium-resolution micrographs do not show clearly whether these cracks are voids or are filled with a thin amorphous tissue. Moreover, a discontinuity of this microstructure is observed in the first 40 nm close to the glass-silicon interface: this part of the layer consists of small isotropic grains, indicative of a distinctive nucleation process in this sample.

We have to note here that nucleation and growth of microcrystalline silicon are critically dependent on the nature of the substrate.[13] Thus, care has to be taken when transferring our observations to layers grown on other substrates. In particular, our observations of the variety of microstructures grown on glass substrates call now for the study of the microstructure of intrinsic μc-Si:H layers grown within p-i-n

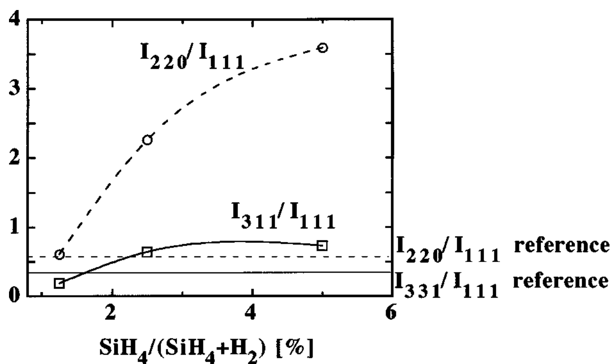

FIG. 7. Variation of the relative peak height compared with the relative peak height of a silicon powder reference sample. The samples close to the amorphous-microcrystalline transition have a marked ⟨220⟩ preferential growth; this texture decreases as the silane concentration decreases.

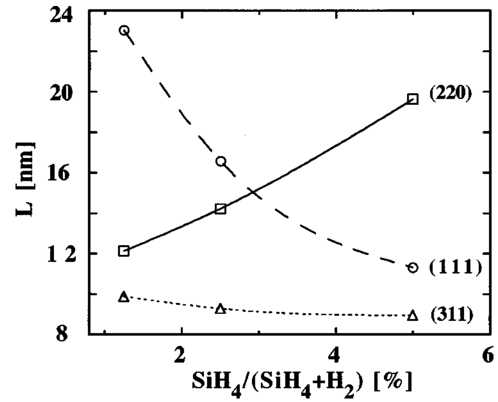

FIG. 8. Variation in the size of the coherent domains as calculated from the extra breadth due to the particule size effect on different diffraction peaks (measured at half peak maximum intensity).

devices. So far all microcrystalline silicon solar cells with efficiencies above 5% have been deposited either at high plasma excitation frequencies in the VHF range[3,14] or at a substrate temperature around 500 °C.[15] To which extent these different deposition conditions all result in a similar common ''optimal microstructure'' of the μc-Si:H layer incorporated in the device is still an open question.

B. Crystallographic texture

Results of x-ray measurements are given in Fig. 6 for the series of samples in which crystallinity was suspected. For silane concentrations $\leqslant 7.5\%$, diffraction peaks are detectable (see magnified inset in Fig. 6). The increase of the total intensity (total peak area) diffracted by the sample with decreasing silane concentration suggests that the crystalline volume fraction increases. However, the exact crystalline volume fraction in each sample cannot be quantified in detail from the diffraction peak area measurements because of the crystallographic texture effects. Each grain in polycrystalline aggregate normally has a crystallographic orientation different from that of its neighbors. Considering all grains as a whole, the orientations of each grain may be distributed randomly, or may tend to cluster around a specific preferential orientation. Any grain aggregate in the latter microstructure is said to have a ''preferred orientation'' or ''preferred orientation'' or ''texture,'' which may be simply defined as a condition in which the crystal orientation is nonrandom. Carefully prepared silicon powder is used as a standard aggregate showing no texture. As indicated in Fig. 7, the relative peak heights measured on our series of samples are different from those published for standard silicon powder.[16] In our case, the ratio of the $I_{(220)}/I_{(111)}$ and the $I_{(311)}/I_{(111)}$ peak heights have been used to monitor the evolution of the crystallographic texture as a function of the silane concentration. Figure 7 shows that ⟨220⟩ is the preferred growth direction. This (220) texture is observed to decrease with decreasing silane concentration. Under the geometrical conditions of the θ–2θ x-ray scan, only those planes parallel to the sample surface (satisfying Bragg's conditions) will contribute to constructive interferences in the direction of reflexion (i.e., towards the x-ray counter). Thus, a preferred ⟨220⟩ orienta-

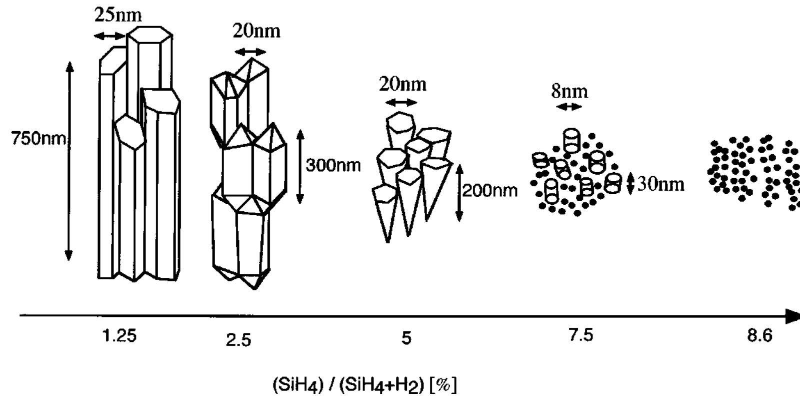

FIG. 9. Schematical picture of the evolution of the microstructure with increasing concentration of silane in hydrogen. The small black dots represent amorphous material. The main information about microstructure given by each measurement technique are indicated: S_q is the root-mean-square surface roughness as determined by atomic force microscopy; the average dimensions and characteristic shape of the crystallites determined from our TEM micrographs are indicated.

tion means that in most of the crystallites the (220) planes are parallel to the sample surface and, hence, the growth of the crystallites occurs by piling up (220) planes. In contrast to that, in the 1.25% silane concentration sample, planes parallel to the sample surface are more randomly distributed.

It is already well known that preferential growth depends strongly on the specific plasma conditions used for deposition. Matsuda *et al.*[17] and Veprek *et al.*[18] have already shown that a variation of the deposition temperature allows one to change from a ⟨111⟩ to a ⟨220⟩ preferential growth direction. It is commonly assumed that those planes being etched away the fastest are also those growing the fastest. However, the detailed mechanism of textured growth in the hydrogen-rich plasma remains unclear and needs further investigations.

C. Grain sizes

One usual way to determine the crystallite grain size is by measuring the broadening of the x-ray diffraction peaks using thereby the Debye–Scherrer equation.[19] In this model, a decreasing grain size leads to an increasing peak width. Note that mechanical stress also leads to an increased peak width, this effect is, however, neglected when simply using the Debye–Scherrer equation. Peak broadening due to sample thickness can be neglected since our samples are around 2 μm thick.[19] The broadening of the three most intense x-ray diffraction peaks has been used for the evaluation of the grain size. The results are plotted in Fig. 8. We observe that $L_{(311)}$ evaluated from the (311) peak width does not vary with the silane concentration, remaining around 10 nm. $L_{(111)}$ and $L_{(220)}$ vary with increasing silane concentration each in an opposite way from 24 down to 12 nm. Note that for an *hkl* reflection, these values $L_{(hkl)}$ are interpreted as the average crystal dimension perpendicular to the reflecting planes. In the geometry of our experiment, it gives, thus, an average dimension of the crystallites in the direction perpendicular to the sample surface. The above-mentioned inverse behavior between $L_{(111)}$ and $L_{(220)}$ with the silane concentration can be attributed mostly to changes in the crystallographic texture as evidenced in Fig. 7. Furthermore, in the Debye–Scherrer equation, an isotropic (cubic) shape of the coherent domains is assumed.[19] This assumption is certainly not true for all the samples in our series: for example, our TEM observations reveal an elongated shape of the grains in the growth direction in all the samples studied. Thus, we can conclude that the variations of $L_{(hkl)}$ in the 24–12 nm range are probably mostly due to both changes in habit plane and to variations of the shape of the grains.

The experimental upper limit for size determination with the Debye–Scherrer equation is of the order of 100–200 nm.[19] From our TEM observations, there is a significant variation of the characteristic features of the microstructure ranging from 100 nm to 1 μm. The Debye–Scherrer method being insensitive to these variations, the observed variations of $L_{(hkl)}$ within the range of 12–24 nm are not an indication of the overall microstructure modifications as observed by TEM. We can conclude that, for the series of samples examined here, x-ray diffraction measurements give useful information on the presence of crystallinity and texture. But x-ray measurements do not constitute an useful source of information about detailed grain sizes and overall grain morphology evolution in our samples.

IV. CONCLUSIONS

We have studied a series of samples deposited by VHF-PECVD with decreasing silane concentration in hydrogen. When the silane concentration is below 8.4%, there is a phase transition between amorphous and microcrystalline silicon, detected both in TEM micrographs and x-ray diffraction measurements. In this series of samples, x-ray diffraction measurements give useful information about the occurrence of the a-Si:H/μc-Si:H phase transition and on the presence of crystallographic texture in the μc-Si:H samples. However, the determination of the coherent domain size from x-ray peak broadening using the Debye–Scherrer equation is only related to the evolution of the smallest microstructural features and, thus, not indicative of the evolution

of the overall microstructure. Indeed, the microstructure as observed by TEM evolves in a complex way from elongated nanocrystals (average diameter of 10 nm and length of 30 nm) embedded in an amorphous tissue towards dendritic growth at intermediate silane concentration and towards long grains (average diameter 20 nm, length 0.7–1 μm) with cracks in between at low silane concentration. The whole picture of the evolution of the layer microstructure with silane concentration is schematically summarized in Fig. 9. The observation of such dramatic microstructural changes in the layers as a function of the plasma phase concentration of silane could not be suspected from the previously published data and demands now a study of the relationship between microstructure and μc-Si:H device performance.

ACKNOWLEDGMENTS

The authors would like to thank Professor M. Morris, Professor F. Stöckli, and Dr. M. Dadras who granted them access to their TEM facilities and S. Dubail for his technical help. The authors also acknowledge the financial support from the Swiss Federal Office for Energy BEW/OFEN under Grants Nos. 2757 and 19431 as well as the Swiss National Science Fund under Grant No. FN52337.

[1] S. Veprek and V. Marecek, Solid-State Electron. **11**, 683 (1968).
[2] J. Meier, R. Flückiger, H. Keppner, and A. Shah, Appl. Phys. Lett. **65**, 860 (1994).
[3] J. Meier *et al.*, Proceedings of the 2nd World Conference and Exhibition on Photovoltaic Solar Energy Conference, Vienna, Austria, 1998, Vol. 1, p. 375.
[4] Y. Chen and S. Wagner, Appl. Phys. Lett. **75**, 1125 (1999).
[5] M. Luysberg, P. Hapke, R. Carius, and F. Finger, Philos. Mag. A **75**, 31 (1997); L. Houben, M. Luysberg, P. Hapke, R. Carius, F. Finger, and H. Wagner, *ibid.* **77**, 1447 (1998).
[6] M. Nakata *et al.*, Mater. Res. Soc. Symp. Proc. **192**, 481 (1990).
[7] U. Kroll, J. Meier, P. Torres, J. Pohl, and A. Shah, J. Non-Cryst. Solids **227–230**, 69 (1998).
[8] U. Kroll *et al.*, J. Appl. Phys. **80**, 4971 (1996).
[9] I. Berbezier, *Porous Silicon Science and Technology* (Les Editions de Physique, Les Ulis, 1994).
[10] M. K. Hatalis and D. W. Greve, J. Appl. Phys. **63**, 2260 (1988).
[11] J. S. Im and R. S. Sposili, MRS Bulletin, March 1996, p. 39, and references therein.
[12] A. Poruba *et al.*, Proceedings of the 2nd World Conference and Exhibition on Photovoltaic Solar Energy Conference, Vienna, Austria, 1998, Vol. 1, p. 781.
[13] J. Koh, Y. Lee, H. Fujwara, C. R. Wronski, and R. W. Collings, Appl. Phys. Lett. **73**, 1526 (1998); J. Koh *et al. ibid.* **75**, 2286 (1999).
[14] K. Saito *et al.*, Proceedings of the 2nd World Conference and Exhibition on Photovoltaic Solar Energy Conference, Vienna, Austria, 1998, Vol. 1, p. 351.
[15] K. Yamamoto *et al.*, Proceedings of the 2nd World Conference and Exhibition on Photovoltaic Solar Energy Conference, Vienna, Austria, 1998, Vol. 2, p. 1284.
[16] ASTM card number 27-1402.
[17] A. Matsuda, K. Kumagai, and K. Tanaka, Jpn. J. Appl. Phys., Part 2 **22**, L34 (1982).
[18] S. Veprek, Z. Iqbal, R. O. Kühne, P. Capezzuto, F. A. Sarott, and J. K. Gimzewski, J. Phys. C **16**, 6241 (1983).
[19] B. D. Cullity, *Elements of X-Ray Diffraction*, 2nd ed. (Addison–Wesley, Reading, MA, 1978), pp. 283 and 284.